Snapshot multi-spectral-line imaging for applications in dermatology and forensics

Janis Spigulis, Ilze Oshina, Peteris Potapovs, Kalvis Lauberts

Janis Spigulis, Ilze Oshina, Peteris Potapovs, Kalvis Lauberts, "Snapshot multi-spectral-line imaging for applications in dermatology and forensics," Proc. SPIE 10881, Imaging, Manipulation, and Analysis of Biomolecules, Cells, and Tissues XVII, 1088114 (4 March 2019); doi: 10.1117/12.2508204

SPIE.

Event: SPIE BiOS, 2019, San Francisco, California, United States

Snapshot multi-spectral-line imaging for applications in dermatology and forensics

Janis Spigulis[1,2], Ilze Oshina[1], Peteris Potapovs[1] and Kalvis Lauberts[2]

[1)] Biophotonics Laboratory, Institute of Atomic Physics and Spectroscopy
[2)] Physics Department, Faculty of Physics, Mathematics and Optometry
University of Latvia, Raina Blvd.19, Riga, LV-1586, Latvia
janis.spigulis@lu.lv

ABSTRACT

Performance of multi-spectral imaging critically depends on image acquisition time and working spectral bandwidths. Ultimate performance can be achieved if a set of monochromatic (single-wavelength) spectral images is obtained by a single snapshot - a technique provisionally called "snapshot multi-spectral-line imaging" or SMSLI. The SMSLI principle and the developed prototype devices for 3, 4 and 5 spectral line snapshot imaging are described. Two potential practical applications of SMSLI are discussed – for fast mapping of the main *in-vivo* skin chromophores and for detection of counterfeit banknotes and documents.
Keywords: spectral imaging, prototype devices for biophotonics, skin chromophore mapping, counterfeit detection.

INTRODUCTION

Two most popular spectral imaging technologies – hyperspectral imaging (HSI) and multispectral imaging (MSI) – are based on sequential capturing of images within relatively narrow spectral bands of typical half-width ~ 10…40 nm. Spectral selectivity is ensured either by spectral band filtering at the image sensor input under "white" (e.g. solar) illumination, or by spectrally narrowband illumination. The first approach is widely used in HSI systems that capture images of the target at tens of adjacent spectral bands. The acquisition process of HSI image set may last a minute or longer[1], so movements of the target area (e.g. *in-vivo* tissue) during the procedure can cause image artefacts. The second approach – spectrally selective illumination – is mainly used in the MSI systems where sequentially switchable non-overlapping spectral bands of illumination (e.g. emitted by several LEDs with different peak wavelengths[2]) are exploited for obtaining the set of spectral images. Advanced MSI systems are portable and self-sustained, much cheaper than HSI systems and better adapted for clinical use; image acquisition procedure is also faster thanks to lower number of the spectral images, typically between 3 and 8. Still, motion artefacts and processing of spectral band images may cause practical problems.

Obviously, both acquisition time of the spectral image set and the spectral bandwidth of each image have to be minimized. Ultimate performance can be achieved if the set of monochromatic (single-wavelength) spectral images is obtained with a single snapshot - a technique provisionally called "snapshot multi-spectral-line imaging" or SMSLI. Worth mentioning that spectral image by definition is an image of target taken at a single working wavelength λ which can be associated with a narrow spectral line. Such image can be obtained under illumination of the target by single spectral line, e.g. by means of a laser illuminator. Using contemporary RGB color cameras, up to three spectral line images can be extracted from a snapshot image data cube at specific illumination that comprises only three spectral lines, each of them positioned within one of the detection bands (R, G or B).[3-5]

Thanks to high spectral purity and fast image acquisition, the SMSLI technology has several promising applications. One of them is distant mapping of skin chromophore distribution. Diagnostics in dermatology critically depends on doctor's visual perception and experience. Lack of affordable equipment, able to quantitatively characterize the malformations, leads to large number of misdiagnoses and unnecessary skin surgeries.[6] Remote mapping of three main skin chromophore (melanin, oxy- and deoxy-hemoglobin) concentration distribution by SMSLI technique[7,8] provides additional information for improved reliability of diagnostics. Also mapping of skin bilirubin, lipids and water is of diagnostic interest; however, simultaneous mapping of four to six chromophores is possible only if the corresponding number of spectral images is available, so more complicated SMSLI technologies have to be developed. This paper

Imaging, Manipulation, and Analysis of Biomolecules, Cells, and Tissues XVII,
edited by Daniel L. Farkas, Attila Tarnok, James F. Leary, Proc. of SPIE Vol. 10881,
1088114 · © 2019 SPIE · CCC code: 1605-7422/19/$18 · doi: 10.1117/12.2508204

briefly reviews our prototype designs for three, four and five spectral line snapshot imaging and discusses the options for eventual future improvements in this area.

Exceptionally high spectral sensitivity of the SMSLI technology makes it attractive for all kinds of color pigment analysis, including counterfeit's detection in forensics. The criminal world rapidly adapts to the existing banknote and document authenticity test equipment, so the tools for counterfeit detection have to be continuously updated using unconventional methods and approaches. The 3-wavelength snapshot imaging, previously used for skin diagnostics, has also shown a promising potential for reliable detection of false banknotes and documents.

1. THE PROTOTYPE DEVICES

A method for extraction of three spectral line images from a single snapshot RGB image data set, taken under simultaneous three-wavelength illumination, has been recently proposed, patent-protected and developed.[3-5] The "win-win" situation was achieved this way – simultaneous acquisition of three target images, all related to extremely narrow spectral intervals (comparable to spectral line FWHM, typically <0.01nm) during a millisecond-range exposure time of the single snapshot. To implement this concept, a smartphone-compatible three spectral line laser illuminator was designed and mounted. Figure 1 shows the illumination scheme (left), design details and outlook of the prototype with smartphone on it (right). Uniform three wavelength (448 nm, 532 nm and 659 nm) illumination of the target area (diameter 40 mm) was ensured by flat ring-shaped laser diffuser. Three pairs of compact 20 mW power laser modules 1 served as light sources; each pair of the equal-wavelength modules was mounted on opposite sides of the 3D-printed cylindrical plastic shielding wall 2. All laser beams were reflected from the 45 degree sloped edge of optical element 3 and turned radial to the diffuser 4. The smartphone was placed on a sticky platform 5 with a round window for its camera, co-aligned with the internal opening of the illuminating diffuser. The camera window was covered by a film polarizer; another film with orthogonal direction of polarization covered the diffuser 4 from bottom, so detection of target surface-reflected light was eliminated. Smartphone model *Google Nexus5* with 8Mpx image sensor *SONY IMX179* was used, ensuring the spatial resolution < 0.1 mm. More details on this device can be found in Ref.8.

The single-snapshot RGB technique is not applicable for express-mapping of more than three skin chromophores. We proposed the double-snapshot approach for fast obtaining 4, 5 or 6 monochromatic images.[9] The idea lies in using up to six different spectral line emitters (e.g. lasers), where three of them are illuminating the target during the first snapshot and some other combination of three illumination lines is used during the second snapshot which follows in less than a second. This concept was first implemented in a model device comprising hand-switchable four laser illuminator and a smartphone. Fig. 2 shows the design scheme and outlook of a smartphone add-on illuminator intended for mapping of four skin chromophores, e.g., melanin, oxy-hemoglobin, deoxy-hemoglobin and bilirubin. Two of the laser modules could be manually re-switched, so providing two sets of 3-wavelengths illumination (405, 532, 650 nm and 450, 532, 650 nm). Four rechargeable AA-type batteries were used for power supply. Relatively uniform illumination of a round

Fig. 1. Optical scheme of the 3-wavelength laser add-on illuminator (left), its design scheme (right, a) and the mobile prototype with smartphone on it (right, b): 1 – laser modules (3 pairs, 448-532-659 nm), 2 – shielding cylinder, 3 – collector of laser beams, 4 – flat ring-shaped light diffuser, 5 – sticky platform for the smartphone, 6 – electronics compartment.

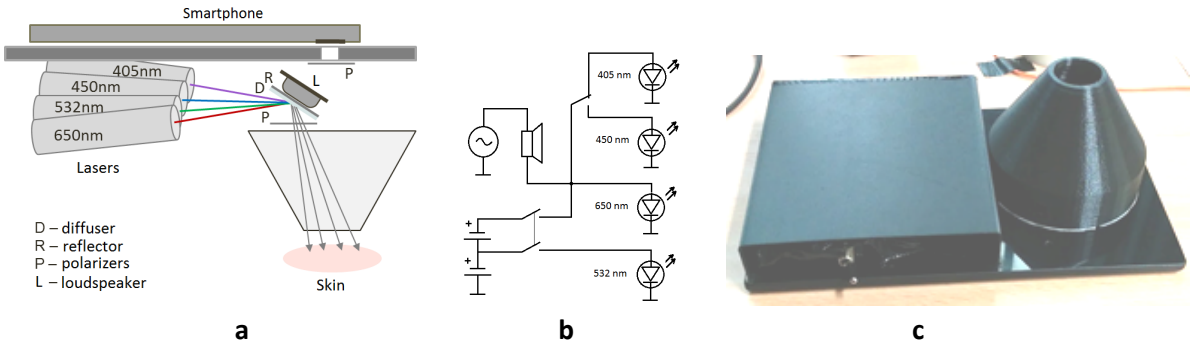

Fig. 2. Design scheme (a), electronic circuit (b) and outlook (c) of the prototype for manually switchable 4-wavelengths skin illumination.

spot (dia. 18 mm) was provided by an advanced optical design which also reduced laser speckle artefacts by means of loudspeaker–initiated vibrations.[10]

As the next step, a portable self-sustained automatically switchable 5-wavelength (405 nm, 448 nm, 532 nm, 659 nm and 842 nm) laser illuminator of similar design, additionally equipped with own NIR-sensitive CMOS camera, Rapsberry Pi3 processing unit and 3.5' touch screen, has been designed and assembled (Fig.3). Two consequent RGB snapshots were taken for spectral image acquisition: the first when 405 nm, 532 nm and 659 nm lasers are switched on and the second when 448 nm, 532 nm and 842 nm lasers are switched on.

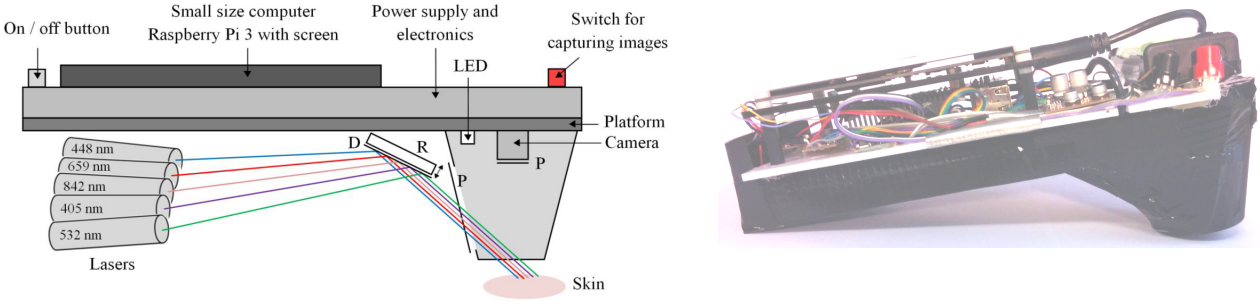

Fig. 3. Design scheme (a) and outlook (b) of the 1st prototype imaging device with automatically switchable 5-wavelengths skin illumination: R – reflector, D – diffuser, P – polarizers.

Fig. 4. The front and rear views of the 2nd prototype for obtaining 5 spectral line images.

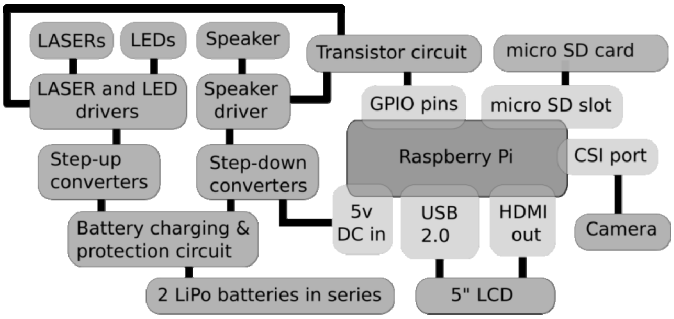

Fig. 5. Functional scheme of the 2nd prototype for obtaining five spectral line images.

This design concept was further developed, introducing 5-wavelength laser diode ring as a light source (which ensured better uniformity of skin illumination at all wavelengths) and white LED illumination for capturing skin color images. The 2nd prototype version also comprised a larger (5 inch) display as shown on Figure 4.

Cornerstone of this device was the Raspberry Pi mini-computer (Figure 5). It captured the images taken with a camera module comprising NIR-sensitive OmniVision OV5647 image sensor and saved the images to microSD card that also comprised the operating system of the device. Five different wavelength laser diodes (405 nm, 450 nm, 520 nm, 660 nm, 850 nm) where used for illumination; extra white LED source ensured correct pointing to the region of interest under a display control. To decrease probability of laser speckle detection, a vibrating speaker was attached to the diffuser. Drivers ensured proper functioning of lasers, white LED and speaker. Each driver worked at different specific voltage, so a switching mode power supply for each driver and individual control was provided. The Raspberry Pi was not able to meet the power demands for the drivers from its GPIO pins, so a transistor circuit was used. Two 5Ah lithium-polymer batteries (in series) served as power supply with appropriate charging and protection circuit. LCD screen was connected via HDMI and powered via USB. Two external pushbutton switches were added for convenience - one for image capturing and the other for power control. The Raspberry Pi device had a version of Raspbian operating system installed. On boot-up it launched Python script that held the necessary information for device to work properly.

Based on the gained experience, currently a new design concept is being implemented in a prototype device under development. Six images of skin malformation will be taken for further analysis using a ring-shaped illumination source, comprising a white LED and five sets of four equal laser diodes emitting at wavelengths 405 nm, 450 nm, 520 nm, 660 nm and 850 nm (or close to these wavelengths). Emission stability will be controlled by internal photodiode, and all necessary measures will be taken to provide uniform and power-equalized illumination of the target at all wavelengths, with reduced skin surface reflection and laser speckle artefacts in the captured images. Three sequential, automatically switchable operation modes will be used: 1) capture of skin color image at white LED illumination, 2) snapshot capture of four spectral line reflection images, 3) capture of autofluorescence image at 405 nm excitation. Combination of multispectral and fluorescent imaging would ensure better specificity of skin cancer identification.[11] The device will be cable-free; image processing will be performed either by an internal mini-computer or by external PC using wireless communication.

3. SPECTRAL LINE IMAGE PROCESSING

If the target is skin and its surface reflection is suppressed, variations in the chromophore composition induce changes in the diffusely reflected light intensities at each of the fixed wavelengths. Such variations in the pathology region relatively to the healthy skin can be quantified by comparing reflected light intensities from equally sized regions of interest in the pathology (I_j) and the adjacent healthy skin (I_{oj}) at each spectral line image. The ratios I_j/I_{jo} can be further transferred into the concentration increase or decrease of all three regarded chromophores Δc_i (i = a, b, c), which can be mapped over the whole image area exploiting the system of equations based on the Beer's law:

$$\begin{cases} \ln\left(\frac{I_1}{I_{01}}\right) = -l_1\left(\Delta c_a \cdot \varepsilon_a(\lambda_1) + \Delta c_b \cdot \varepsilon_b(\lambda_1) + \Delta c_c \cdot \varepsilon_c(\lambda_1)\right) \\ \ln\left(\frac{I_2}{I_{02}}\right) = -l_2\left(\Delta c_a \cdot \varepsilon_a(\lambda_2) + \Delta c_b \cdot \varepsilon_b(\lambda_2) + \Delta c_c \cdot \varepsilon_c(\lambda_2)\right) \\ \ln\left(\frac{I_3}{I_{03}}\right) = -l_3\left(\Delta c_a \cdot \varepsilon_a(\lambda_3) + \Delta c_b \cdot \varepsilon_b(\lambda_3) + \Delta c_c \cdot \varepsilon_c(\lambda_3)\right) \end{cases} \quad (1),$$

where $\varepsilon_i(\lambda_j)$ - extinction coefficients of three regarded chromophores at three exploited wavelengths, l_j – absorption path length in skin at a particular wavelength. Chromophore concentration increase or decrease at each selected group of pixels is found by solving the linear equation system (1) with abbreviated measured quantities $k_j = \ln(I_j/I_{jo})$:

$$\begin{aligned} \Delta c_a &= A_1 \cdot k_1 + A_2 \cdot k_2 + A_3 \cdot k_3 \\ \Delta c_b &= B_1 \cdot k_1 + B_2 \cdot k_2 + B_3 \cdot k_3 \\ \Delta c_c &= C_1 \cdot k_1 + C_2 \cdot k_2 + C_3 \cdot k_3 \end{aligned} \quad (2).$$

Distribution of the changed chromophore concentrations can be then mapped; see more details in Ref.8.

The triple-wavelength device was also used for comparative analysis of genuine and counterfeit banknotes, in order to assess the potential of SMSLI technology for detection of colored counterfeits. Scheme for processing of the banknote spectral line images is presented in Figure 6,a. If necessary, over-exposure corrections were performed after the spectral line image acquisition, and then three working images of the same spot were mutually divided or extracted. For each pixel group (related to a specific spot on banknote) a parameter called k-factor was calculated as ratio of mean values of the informative and the background pixels (as illustrated on Fig. 6,b). Comparison of k-values further served for distinguishing between authentic and false banknotes.

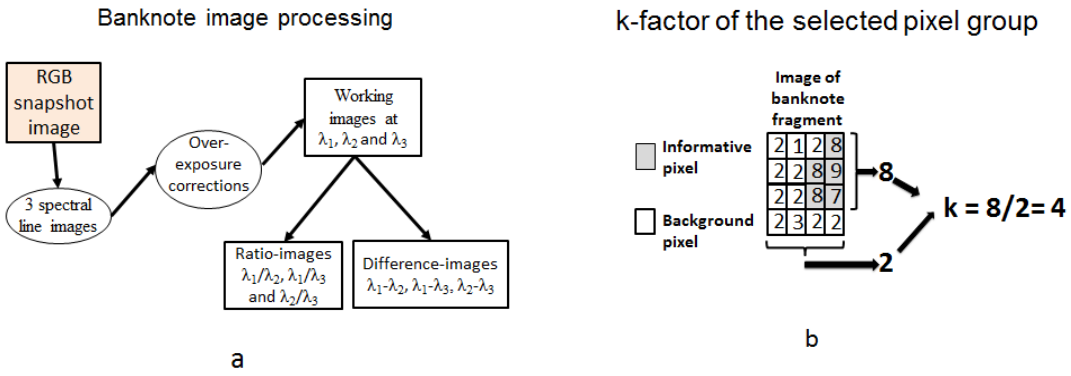

Fig. 6. Processing scheme of the banknote spectral images (a) and illustration for k-factor calculation of a selected pixel group (b).

4. POTENTIAL APPLICATIONS

4.1. Mapping of skin chromophore distribution

Our triple-wavelength laser illuminator prototype (Fig.1) allowed obtaining physiologically plausible chromophore distribution maps in pigmented and vascular skin lesions by a single snapshot. Several tens of various skin malformations (diagnosed by a certified dermatologist) were examined under approval of local ethics committee with written consent of the volunteers. Figure 7 illustrates how melanin content increases in a pigmented nevus (upper raw), without essential changes in the hemoglobin content. Similar response was observed for another pigmented skin malformation – seborrheic keratosis (middle raw). Quite different chromophore composition changes were recorded for vascular hemangiomas (lower raw) – melanin concentration in the pathology remained practically unchanged while the oxy-hemoglobin content notably increased and the deoxy-hemoglobin content decreased in comparison to the healthy

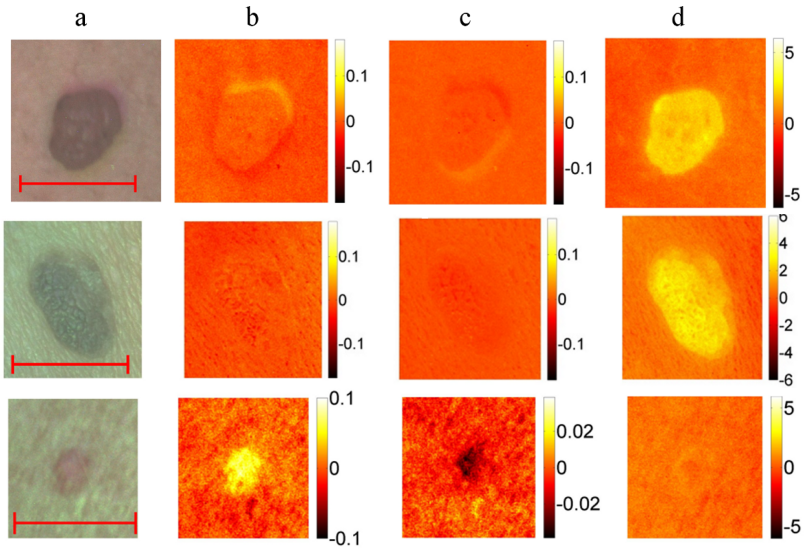

Fig. 7. Clinical color RGB images (a, scale bar 5 mm) and the corresponding chromophore distribution maps for three skin pathologies: pigmented nevus (upper raw), seborrheic keratosis (middle raw) and vascular hemangioma (lower raw); b – oxy-hemoglobin, c – deoxy-hemoglobin, d – melanin. Units of the color scale – mili-moles[8].

surrounding skin. These correlations confirm the potential of the SMSLI technology for quantifying dermatologist's diagnosis taking into account the relative chromophore concentration changes in the malformation relatively to healthy skin.

4.2. Spectral line imaging of authentic and counterfeit banknotes.

Altogether 58 authentic and counterfeit 20 EUR and 50 EUR banknotes were examined using the triple-wavelength prototype (Fig.1). The taken out of circulation false banknotes (with identified counterfeit method) were kindly provided by the Money Technology Department of the Bank of Latvia – see table 1 for more details.

Table 1. The examined EUR 20 and EUR 50 banknotes.

	Authentic	**Counterfeit**			
		Jet-printed	Offset-printed	Color-copied	Other
EUR 20 (new version)	7	2	-	2	3
EUR 20 (old version)	2	-	10	-	3
EUR 50 (new version)	15	1	-	-	2
EUR 50 (old version)	3	-	1	-	7
In total:	**58**				

If comparing the exploited three wavelengths, the highest sensitivity for counterfeit detection exhibited the blue 448nm spectral line images – see Figure 8 for illustration. Spectral line image ratios involving 448 nm images appeared to be even more sensitive (Figure 9).

a b c

Fig. 8. Sample of 20 EUR banknote with marked RoI (a) and its 448 nm images for authentic (b) and counterfeit (c) banknotes.

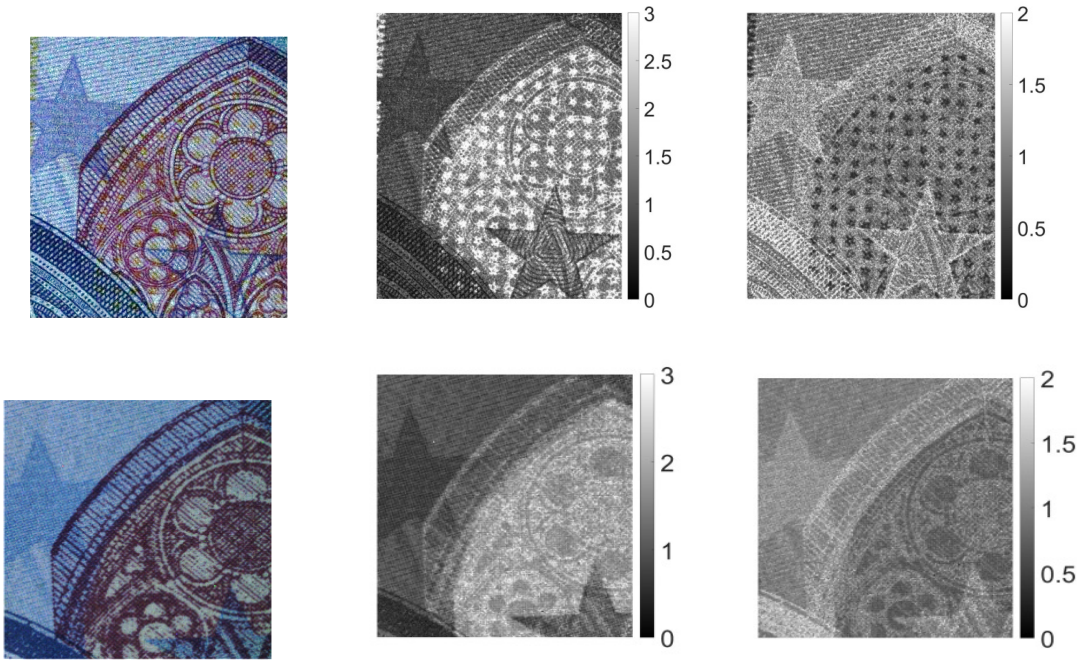

RGB 659nm/448nm 448nm/532nm

Fig. 9. Comparison of RGB images and spectral line image ratios for the same fragment of authentic (upper raw) and counterfeit (lower raw) 20 EUR banknotes.

Also the k-factor statistical analysis confirmed the advantages of blue spectral line images compared to the other two (green $\lambda G = 532$ nm and red $\lambda R = 659$ nm), as well as of the spectral line image ratios with involvement of $\lambda B = 448$ nm images. Figure 10 illustrates this for the case of equal fragments of the 50 EUR banknotes – authentic, counterfeit by jet-printing and counterfeit by another (non-identified) method. One can see that the red line images are less sensitive to counterfeit while the green line images, as well as image ratios and differences with involvement of green images still show ability to distinguish the counterfeit.

The above results show that SMSLI technology may be well-adapted for fast banknote counterfeit detection; however, much more comprehensive studies are needed to implement this technology in routine forensics. The same relates to counterfeit document (e.g. agreements, identification cards, driver's licences) detection – our preliminary results showed that not only colored items but even black prints on white paper produced by different laser printers can be distingushed using the triple-wavelengths image analysis.

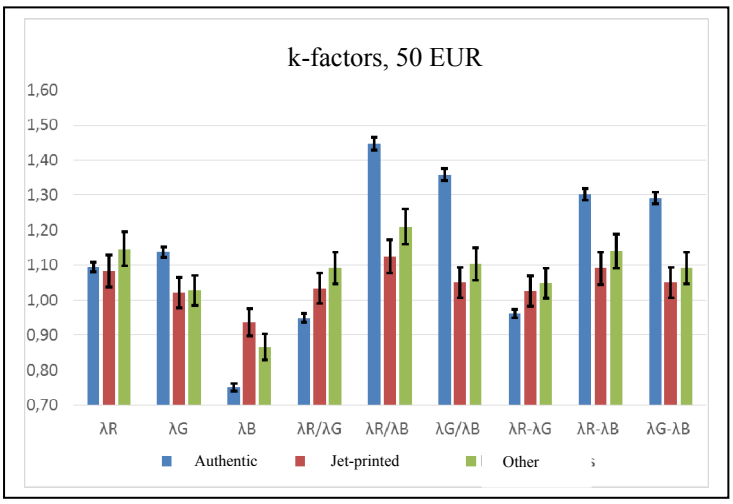

Fig. 10. The calculated k-factors for the same fragment of three 50 EUR banknotes – authentic and two counterfeits (jet-printed and uncategorized).

5. SUMMARY

The proposed and experimentally examined SMSLI technique exhibits two distinct advantages if compared with conventional spectral imaging approaches (e.g. HSI, MSI) – better spectral selectivity and shorter acquisition time. It opens new challenges for color pigment analysis in several areas of application, including dermatology (mapping of skin chromophore concentration changes in pigmented and vascular malformations) and forensics (detection of counterfeit banknotes and documents by comparative analysis of spectral line images and their ratios). So far the application potential has been confirmed in studies using the 3-wavelength technique - snapshot RGB imaging under triple laser line illumination; currently more advanced 4-6 wavelength snapshot imaging methods and devices are being developed. In general, the SMSLI technology promises increased accuracy and reliability both for diagnostic and forensic applications.

ACKNOWLEDGEMENTS

Financial support provided by the Latvian Council of Science (grant # lzp-2018/2-0006) is highly appreciated. Forensic research was inspired and supported by the EC COST action CA16101 “Multiforesee”.

REFERENCES

[1] Kuzmina I., Diebele I, Spigulis J, Valeine L, Berzina A, Abelite A., “Contact and contactless diffuse reflectance spectroscopy: potential for recovery monitoring of vascular lesions after intense pulsed light treatment,” *J. Biomed. Opt.*, **16**(4), 040505 (2011).

[2] Kapsokalyvas D., Bruscino N., Alfieri D., de Giorgi V., Cannarozzo G., Cicchi R., Massi N., Pimpinelli N., Pavone F.S., “Spectral morphological analysis of skin lesions with a polarization multispectral dermoscope,” *Opt. Express* **21**(4),4826-40 (2013).

[3] WO 2013135311 A1 (2012), “Method and device for imaging of spectral reflectance at several wavelength bands”.

[4] Spigulis J., Elste L., “Single-snapshot RGB multispectral imaging at fixed wavelengths: proof of concept”, *Proc. SPIE* **8937**, 89370L (2014).

[5] Spigulis J., “Multispectral, fluorescent and photoplethysmographic imaging for remote skin assessment”, *Sensors* **17**, 1165 (2017).

[6]] Lin M.J., Mar V., McLean C., Wolfe R., Kelly J. W, “Diagnostic accuracy of malignant melanoma according to subtype,” *Australas J. Dermatol*. **55**(1), 35-42 (2013).

[7] Spigulis J., Oshina I.. Snapshot RGB mapping of skin melanin and hemoglobin. *J.Biomed.Opt*., **20**(5), 050503 (2015).

[8] Spigulis J., Oshina I., Berzina A., Bykov A., “Smartphone snapshot mapping of skin chromophores under triple-wavelength laser illumination”, *J.Biomed.Opt.*, **22**(9), 091508 (2017).

[9] LV 15106 B (2016), “Method and device for mapping of chromophores under illumination by several laser lines”.

[10] WO 2018/177565 A1 (2018), “Device for speckle-free imaging under laser illumination”.

[11] Lihachev A., Lihacova I., Plorina E.V., Lange M., Derjabo A., Spigulis J., “Differentiation of seborrheic keratosis from basal cell carcinoma, nevi and melanoma by RGB autofluorescence imaging”, *Biomed.Opt.Expr.,* **9**(4), 1852-1858 (2018).